

Adiabatic Lapse Rate and Static Stability in the Venus Atmosphere calculated from Real Gas Mixture Models

Arkopal Dutt^{a,1,*}, Sanjay S. Limaye^a

^a*Space Science and Engineering Center, University of Wisconsin-Madison, Madison, WI 53706, USA*

Abstract

It is known that the ideal gas equation of state is not valid in the lower atmosphere of Venus where surface pressures reach 9 MPa and surface temperatures approach 750 K. Moreover, the presence of a small amount of nitrogen slightly complicates the calculation of thermodynamic properties of the real gas mixture present in the atmosphere. Previous calculations of the adiabatic lapse rate in the Venus atmosphere have used approximations to estimate the adiabatic lapse rate. Here, we calculate the adiabatic lapse rate more accurately by using multi-parameter mixture models formulated in reduced Helmholtz free energy to account for the real gas mixture effects. Our results show small differences from the [Seiff et al. \(1980\)](#) values for the adiabatic lapse rate which may be significant where the Venus atmosphere is close to being neutral. For accurate knowledge of the static stability for atmosphere circulation, a local value of the adiabatic lapse rate is necessary.

Keywords: Venus; Atmospheres, composition; Atmospheres, structure;

1. Introduction

[Staley \(1970\)](#) pointed out that the adiabatic lapse rate for the lower atmosphere of Venus cannot be calculated using the ideal gas equation (g/c_p) due to the high temperature and pressure conditions and the presence of small amount of nitrogen. Considering an arbitrary equation of state for any gas mixture, [Staley \(1970\)](#) derived the following expression for adiabatic lapse rate Γ at the altitude z in a planetary atmosphere

$$\Gamma = -\frac{dT}{dz} = -\frac{T}{\rho} \frac{\left(\frac{\partial p}{\partial T}\right)_\rho}{\left(\frac{\partial p}{\partial \rho}\right)_T} \left(\frac{g}{c_p}\right) = \frac{T}{\rho} \left(\frac{\partial \rho}{\partial T}\right)_p \left(\frac{g}{c_p}\right) \quad (1)$$

where T is temperature, p is pressure, ρ is the density, g is the acceleration due to gravity and c_p is the isobaric specific heat capacity of the air at altitude z . Assuming that the atmosphere is composed of pure CO_2 , [Staley \(1970\)](#) calculated c_p and hence Γ using the real gas physical properties of pure CO_2 ([Hilsenrath et al., 1955](#)) across a range of pressure and temperature that can be found in the atmosphere of Venus. The major shortcoming of this approach was that the presence of N_2 in the atmosphere was neglected. In order to overcome this, [Seiff et al. \(1980\)](#)

*Corresponding author

Email addresses: arkopal@mit.edu (Arkopal Dutt), sanjayl@ssc.wisc.edu (Sanjay S. Limaye)

¹Present address: Department of Mechanical Engineering, Massachusetts Institute of Technology, Cambridge, MA 02139, USA

calculated the adiabatic lapse rate by assuming an ideal binary gas mixture of real gas components: carbon dioxide (CO_2) and nitrogen (N_2) in a volume measured mixing ratio of 96.5 : 3.5, arguing that the abundance of nitrogen is small. In this approach, adiabatic lapse rate is written as

$$\Gamma = -(aT) \frac{g}{c_p} \quad (2)$$

where

$$a = -\frac{1}{\rho} \left(\frac{\partial \rho}{\partial T} \right)_p \quad (3)$$

In the case of an ideal binary gas mixture, the contribution of pure real gas component i to the thermodynamic properties of the mixture is directly proportional to its mole fraction x_i which gives

$$c_p = \sum_i x_i c_{pi} \quad (4)$$

$$aT = \sum_i x_i (aT)_i \quad (5)$$

The main drawback of this method is that the non-ideal interactions of CO_2 and N_2 in the mixture are neglected in calculating the thermodynamic properties of the mixture.

Furthermore, the VIRA model (Seiff et al., 1985) extrapolated the surface temperature of Venus below 12 km altitude (at which the last measurements were made by the sensors on the four Pioneer probes) by using the adiabatic lapse rate calculated by Seiff et al. (1980). Thus surface temperatures reported for all Pioneer probes are slightly inaccurate. As a result, the values calculated for the surface conditions on Venus which has been used in most subsequent studies pertaining to the stability of atmosphere and atmospheric circulation can be made more accurate. VeGa2 lander is the only atmospheric probe which has provided us with accurate measurements down to the surface. VeGa2 lander data in the lower atmosphere was examined by Team and Seiff (1987) which showed near neutral and superadiabatic layers. Presence of superadiabatic layers on Venus raises some key questions about the source of near surface heat deposition and the resulting atmospheric circulation in the lower atmosphere. An important parameter in understanding such atmospheric processes on Venus is static stability which influences small-scale turbulence caused by convection or wind shear, mesoscale motions and large-scale circulations as well as topography induced disturbances by the ambient flow. Thus it is imperative to calculate the adiabatic lapse rate accurately for the known conditions on Venus.

A more detailed derivation of the real gas adiabatic lapse rate for a planetary atmosphere with a multi-component real gas mixture composition varying with altitude is illustrated in Appendix A. The same expressions for adiabatic lapse rate (Eqs.1) as originally derived by Staley (1970) are obtained. As can be seen from the expressions, accuracy in adiabatic lapse rate at any altitude depends on the accuracy in Venus atmosphere profiles available, composition of the atmosphere at that altitude, density ρ and the isobaric specific heat capacity c_p of air at that altitude. As there is limited experimental data available for the particular real gas binary mixture that largely makes up the Venus atmosphere, it becomes necessary to use an equation of state to predict the density ρ and isobaric specific heat capacity c_p at different pressures p and temperatures T . We have already highlighted how the approaches followed by both Staley (1970) and Seiff et al. (1980) introduced errors in the determination of these quantities for the real gas binary mixture of $CO_2 - N_2$ that largely make up the Venus atmosphere.

In this work, we determine ρ and c_p more accurately than previous approaches by considering the interactions between real gas components in the mixture through a equation of state for the mixture. A variety of different equations of state for fluids and mixtures exist (Sengers et al., 2000). Here, we determine the physical properties of the real gas binary mixture $CO_2 - N_2$ by using thermodynamic models in Helmholtz energy. We consider two different Helmholtz energy mixture models proposed in (Lemmon and Jacobsen, 1999) and (Kunz and Wagner, 2012). The advantage these models present over other equations of state for mixtures is that it allows us to obtain the mixture properties by combining properties of real gas components obtained through their respective equations of state. In Sections 2 and 3, we review these models and how they can be used to calculate the desired thermodynamic quantities. This will be followed by a verification of the approach against experimental data and prior approaches in Section 4. In Section 5, we show how the mixture models can be used to calculate the adiabatic lapse rate and static stability for the Venus atmosphere. Results are discussed in Section 6. Finally in Section 7, we highlight the results obtained and discuss future work.

2. Background

2.1. Review of Mixture Models

Equations of state formulated in reduced Helmholtz free energy for mixtures were first proposed independently by Tillner-Roth (1993) and Lemmon (1996). These empirical multi-parameter models rely on mixing rules to obtain properties of multi-component mixtures from equations of states of the pure fluid components. These mixing rules and the equations of state of the pure fluid components themselves are obtained through fitting of experimental data of multiple thermodynamic properties. The first mixture model that we consider was proposed in (Lemmon and Jacobsen, 1999). The second mixture model that we consider is the GERG-2008 model which was proposed in (Kunz and Wagner, 2012) and is considered the most accurate mixture model for obtaining thermodynamic properties of natural gases. The older GERG-2004 mixture model (Kunz et al., 2007) was used by Hagermann et al. (2007) to estimate the abundance of methane in Titan’s atmosphere using speed of sound measurements through a Bayesian analysis. However, mixture models in Helmholtz energy have not been applied to compute adiabatic lapse rate of a multi-component planetary atmosphere before.

A more recent mixture model was proposed in (Gernert, 2013) to predict thermodynamic properties mixtures relevant for Carbon Capture Storage more accurately. However, the mixing rule suggested for the binary mixture of carbon dioxide and nitrogen in (Kunz and Wagner, 2012) remains unchanged. We consider the two different mixture models to reflect the effect of mixing rules on accuracy even when both models use the same pure fluid equations of state. From here on, we will refer to the mixture model introduced in (Lemmon and Jacobsen, 1999) as LJ-1999 model and Seiff et al. (1980) approach of considering ideal mixture of real gases as IMRG model.

2.2. Mixture Model in Helmholtz Free Energy

Any generalized mixture model in Helmholtz free energy A with independent mixture variables ρ , temperature T and molar composition \bar{x} (Lemmon, 1996; Lemmon and Jacobsen, 1999; Kunz and Wagner, 2012) can be written as

$$A(\tilde{\rho}, T, \bar{x}) = A^{idmix}(\tilde{\rho}, T, \bar{x}) + A^E(\tilde{\rho}, T, \bar{x}) \quad (6)$$

where A^{idmix} is the Helmholtz energy of the ideal mixture of the real gas components, A^E is the Helmholtz energy contribution to mixing, $\tilde{\rho}$ ($= \rho/M$) is the amount of substance density and M is

the molar mass of the mixture. In general, $M = \sum_i x_i M_i$ where M_i is the molar mass of component i . [Seiff et al. \(1980\)](#) essentially neglected A^E in calculating c_p in Eq.4. It is however easier to work with the following decomposition of the Helmholtz energy of the mixture

$$A(\tilde{\rho}, T, \bar{x}) = A^o(\tilde{\rho}, T, \bar{x}) + A^r(\tilde{\rho}, T, \bar{x}) \quad (7)$$

where A^o is the contribution of the ideal gas and A^r is the contribution from the residual Helmholtz energy of the pure fluid components and from the Helmholtz energy contribution to mixing. Non-dimensionalizing Eq.7 by dividing by RT ($R = 8.314510 \text{ J}/(\text{mol}\cdot\text{K})$ is the universal gas constant and T is the mixture temperature), we obtain

$$\alpha(\tilde{\rho}, T, \bar{x}) = \alpha^o(\tilde{\rho}, T, \bar{x}) + \alpha^r(\delta, \tau, \bar{x}) \quad (8)$$

where δ is the reduced mixture density and τ is the inverse reduced mixture temperature given by

$$\delta = \tilde{\rho}/\rho_r(\bar{x}) \quad (9)$$

$$\tau = T_r(\bar{x})/T \quad (10)$$

These reducing parameters are only functions of the composition as indicated above. They are specific to the mixing rule that is followed. For example, the reducing function used in the Lemmon's model ([Lemmon and Jacobsen, 1999](#)) is very different from that used in the GERG-2008 model ([Kunz and Wagner, 2012](#)). The non-dimensionalized Helmholtz free energy of the ideal gas mixture is

$$\frac{A^o(\tilde{\rho}, T, \bar{x})}{RT} = \alpha^o(\tilde{\rho}, T, \bar{x}) = \sum_{i=1}^n x_i [\alpha_i^o(\tilde{\rho}, T) + \ln x_i] \quad (11)$$

where α_i^o is the ideal gas Helmholtz energy of component i in the mixture which is a function of the mixture amount of substance density $\tilde{\rho}$ and temperature T , and not that of reduced density δ and inverse reduced temperature τ . The term $\sum_{i=1}^n x_i \ln x_i$ quantifies the entropy of mixing. The residual part of the non-dimensionalized Helmholtz free energy is

$$\frac{A^r}{RT} = \alpha^r = \sum_{i=1}^n x_i \alpha_i^r(\delta, \tau) + \alpha^E(\delta, \tau, \bar{x}) \quad (12)$$

where α_i^r is the non-dimensionalized residual part of Helmholtz free energy of component i in the mixture and α^E is called the excess value of the non-dimensionalized Helmholtz free energy or the departure function ([Kunz and Wagner, 2012](#)). The usual functional form is

$$\alpha^E(\delta, \tau, \bar{x}) = \sum_{i=1}^{n-1} \sum_{j=i+1}^n x_i x_j F_{ij} \alpha_{ij}^r(\delta, \tau) \quad (13)$$

where the functional form of α_{ij}^r and the value of parameter F_{ij} is prescribed by the mixing rule being used. All common thermodynamic properties such as pressure, isochoric heat capacity, isobaric heat capacity, sound of speed, enthalpy, saturated-liquid density and VLE data can be obtained from the derivatives of α^o and α^r . A list of the expressions can be found in ([Kunz and Wagner, 2012](#)). Here, we only list those that are of relevance to us

$$p = \tilde{\rho}RT \left[1 + \delta \left(\frac{\partial \alpha^r}{\partial \delta} \right)_{\tau} \right] \quad (14)$$

$$\frac{\tilde{c}_v}{R} = -\tau^2 \left[\left(\frac{\partial^2 \alpha^0}{\partial \tau^2} \right) + \left(\frac{\partial^2 \alpha^r}{\partial \tau^2} \right)_\delta \right] \quad (15)$$

$$\frac{\tilde{c}_p}{R} = \frac{\tilde{c}_v}{R} + \frac{\left[1 + \delta \left(\frac{\partial \alpha^r}{\partial \delta} \right)_\tau - \delta \tau \left(\frac{\partial^2 \alpha^r}{\partial \delta \partial \tau} \right) \right]^2}{1 + 2\delta \left(\frac{\partial \alpha^r}{\partial \delta} \right)_\tau + \delta^2 \left(\frac{\partial^2 \alpha^r}{\partial \delta^2} \right)_\tau} \quad (16)$$

To complete the mixture model setup, we still need to specify the mixing rules in order to evaluate the reduced mixture density δ , reduced mixture temperature τ and the departure function α^E . We also need to specify the equations of state for CO_2 and N_2 that we will use to calculate the ideal Helmholtz energy α_i^0 , residual Helmholtz energy α_i^r and their derivatives. One reason for considering LJ-1999 mixture model and the GERG-2008 mixture model is that they both consider the same set of equations of state for the pure components of CO_2 and N_2 .

2.2.1. LJ-1999 Mixture Model

As mentioned before, a mixing rule specifies how the equations of state of the pure components will be combined to evaluate the properties of the mixture. Firstly, we require the evaluation of the reduced mixture density and temperature which depend on the expressions of the reducing functions of density and temperature. For the LJ-1999 mixture model, they are given by

$$\rho_r = \left[\sum_{i=1}^n \frac{x_i}{\tilde{\rho}_{ci}} + \sum_{i=1}^{n-1} \sum_{j=i+1}^n x_i x_j \xi_{ij} \right]^{-1} \quad (17)$$

$$T_r = \sum_{i=1}^n x_i T_{ci} + \sum_{i=1}^{n-1} \sum_{j=i+1}^n x_i^{\beta_{ij}} x_j^{\phi_{ij}} \zeta_{ij} \quad (18)$$

where $\tilde{\rho}_{ci}$ is the critical amount of substance density of component i , T_{ci} is the critical temperature of component i , and ξ_{ij} , β_{ij} , ϕ_{ij} and ζ_{ij} are constant parameters particular to the mixture. For a binary mixture, the expressions for reducing values simplify to

$$\rho_r = \left[\frac{x_1}{\tilde{\rho}_{c1}} + \frac{x_2}{\tilde{\rho}_{c2}} + x_1 x_2 \xi_{12} \right]^{-1} \quad (19)$$

$$T_r = x_1 T_{c1} + x_2 T_{c2} + x_1^{\beta_{12}} x_2^{\phi_{12}} \zeta_{12} \quad (20)$$

For the LJ-1999 mixture model, the departure function is given by

$$\frac{A^E}{RT} = \alpha^E = \sum_{i=1}^{n-1} \sum_{j=i+1}^n x_i x_j F_{ij} \sum_{k=1}^{10} N_k \delta^{d_k} \tau^{t_k} \quad (21)$$

The parameters in Eq.21 which are not specific to the mixture are presented in the Table 1. In the case of the binary mixture $CO_2 - N_2$, $F_{12} = 2.780647$, $\xi_{12} = 0.00659978 \text{ dm}^3 \text{ mol}^{-1}$, $\zeta_{12} = -31.149300 \text{ K}$, $\phi_{12} = 1$ and $\beta_{12} = 1$.

k	N_k	d_k	t_k
1	$-0.245476271425 \times 10^{-1}$	1	2
2	-0.241206117483	1	4
3	$-0.513801950309 \times 10^{-2}$	1	-2
4	$-0.239824834123 \times 10^{-1}$	2	1
5	0.259772344008	3	4
6	-0.172014123104	4	4
7	$0.429490028551 \times 10^{-1}$	5	4
8	$-0.202108593862 \times 10^{-3}$	6	0
9	$-0.382984234857 \times 10^{-2}$	6	4
10	$0.262992331354 \times 10^{-5}$	8	-2

Table 1: Parameters for Eq.21

2.2.2. GERG-2008 Model

The mathematical structure of the reducing functions for density and temperature for the GERG-2008 model are more complicated than the LJ-1999 model and are given by

$$\rho_r = \left[\sum_{i=1}^n x_i^2 \frac{1}{\tilde{\rho}_{c,i}^2} + \sum_{i=1}^{n-1} \sum_{j=i+1}^n 2x_i x_j \beta_{v,ij} \gamma_{v,ij} \cdot \frac{x_i + x_j}{\beta_{v,ij}^2 x_i + x_j} \cdot \frac{1}{8} \left(\frac{1}{\tilde{\rho}_{c,i}^{1/3} + \tilde{\rho}_{c,j}^{1/3}} \right)^3 \right]^{-1} \quad (22)$$

$$T_r = \sum_{i=1}^n x_i^2 T_{ci} + \sum_{i=1}^{n-1} \sum_{j=i+1}^n 2x_i x_j \beta_{T,ij} \gamma_{T,ij} \cdot \frac{x_i + x_j}{\beta_{T,ij}^2 x_i + x_j} (T_{c,i} \cdot T_{c,j})^{0.5} \quad (23)$$

where $\beta_{v,12} = 0.977794634$, $\gamma_{v,12} = 1.047578256$, $\beta_{T,12} = 1.005894529$ and $\gamma_{T,12} = 1.107654104$ for the binary mixture of $CO_2 - N_2$. The function α_{ij}^r which is a part of α^E (Eq.13) is given by

$$\alpha_{12}^r(\delta, \tau) = \sum_{k=1}^2 n_k \delta^{d_k} \tau^{t_k} + \sum_{k=3}^6 n_k \delta^{d_k} \tau^{t_k} \cdot \exp \left[-\eta_k (\delta - \epsilon_k)^2 - \beta_k (\delta - \gamma_k) \right] \quad (24)$$

and $F_{12} = 1.0$ for $CO_2 - N_2$. The values of the different parameters in Eq.24 are given in Table 2.

k	d_k	t_k	n_k	η_k	ϵ_k	β_k	γ_k
1	2	1.850	0.28661625028399	0.000	0.000	0.000	0.000
2	3	1.400	-0.10919833861247	0.000	0.000	0.000	0.000
3	1	3.200	-1.13740320822700	0.250	0.500	0.750	0.500
4	1	2.500	0.76580544237358	0.250	0.500	1.000	0.500
5	1	8.000	0.00426380009268	0.000	0.500	2.000	0.500
6	2	3.750	0.17673538204534	0.000	0.500	3.000	0.500

Table 2: Parameters for Eq.21

2.3. Equation of State for CO_2 and N_2

For the pure fluids of carbon dioxide CO_2 and nitrogen N_2 , we use the equations of state proposed by Span and Wagner (1996) and Span et al. (2000) respectively. As mentioned before, the

LJ-1999 and GERG-2008 mixture models define mixing rules considering these pure fluid equations of state. They are also accurate in a vast temperature and pressure region as can be seen in Table 3. For CO_2 , the equation of state can be extrapolated from the triple-point temperature down to 90 K (Klimeck, 1996; Kunz and Wagner, 2012) without loss in accuracy and we can thus cover the entire range of p and T in the Venus atmosphere.

Substance	Reference	Range of validity		Molar mass [kg·kmol ⁻¹]	T_c [K]	$\tilde{\rho}_c$ [kmol·m ⁻³]
		T [K]	Max. p [MPa]			
CO_2	Span and Wagner (1996)	216 – 1100	800	44.0098	304.1282	10.6249
N_2	Span et al. (2000)	63.151 – 1000	2200	28.01348	126.192	11.1839

Table 3: References and critical parameters of CO_2 and N_2

The equation of state for the pure fluids is explicit in the dimensionless Helmholtz energy α using independent variables of reduced density and temperature.

$$\frac{A_i(\rho, T)}{RT} = \alpha_i(\delta, \tau) = \alpha_i^o(\delta, \tau) + \alpha_i^r(\delta, \tau) \quad (25)$$

where the subscript i denotes the component of interest (i.e. CO_2 or N_2). In the above equation, δ is the mixture reduced density and τ is the mixture reduced temperature when calculating the contribution of component i to any mixture. When calculating the Helmholtz energy for a system containing only the pure fluid i , $\delta = \tilde{\rho}/\tilde{\rho}_c$ and $\tau = T_c/T$. This would also be obtained from the reducing functions of Eqs.17 and 18 for the LJ-1999 mixture model or Eqs.23 and 22 for the GERG-2008 mixture model respectively

Nitrogen. The ideal gas Helmholtz energy of N_2 is given by

$$\alpha_{N_2}^o(\delta, \tau) = \ln \delta + a_1 \ln \tau + a_2 + a_3 \tau + a_4 \tau^{-1} a_5 \tau^{-2} + a_6 \tau^{-3} + a_7 \ln[1 - \exp(-a_8 \tau)] \quad (26)$$

where $a_1 = 2.5$, $a_2 = -12.76953$, $a_3 = -0.007841630$, $a_4 = -1.934819 \times 10^{-4}$, $a_5 = -1.247742 \times 10^{-5}$, $a_6 = 6.678326 \times 10^{-8}$, $a_7 = 1.012941$ and $a_8 = 26.65788$. The residual gas Helmholtz energy of N_2 is given by

$$\alpha_{N_2}^r(\delta, \tau) = \sum_{k=1}^6 N_k \delta^{i_k} \tau^{j_k} + \sum_{k=7}^{32} N_k \delta^{i_k} \tau^{j_k} \exp(-\delta^{l_k}) + \sum_{k=33}^{36} N_k \delta^{i_k} \tau^{j_k} \exp(-\psi_k (\delta - 1)^2 - \beta_k (\tau - \gamma_k)^2) \quad (27)$$

The derivatives of $\alpha_{N_2}^r$ as required in the mixture model and values of the parameters N_k , i_k , j_k , l_k , ψ_k , β_k , and γ_k (for different values of k) are given in Appendix B.

Carbon Dioxide. Ideal Helmholtz energy is given by

$$\alpha_{CO_2}^o(\delta, \tau) = \ln \delta + a_1^0 + a_2^0 \tau + a_3^0 \ln \tau + \sum_{i=4}^8 a_i^0 \ln[1 - \exp(-\tau \theta_i^0)] \quad (28)$$

i	a_i^0	θ_i^0	i	a_i^0	θ_i^0
1	8.37304456		5	0.62105248	6.11190
2	-3.70454304		6	0.41195293	6.77708
3	2.50000000		7	1.04028922	11.32384
4	1.99427042	3.15163	8	0.08327678	27.08792

Table 4: Parameters as in Eq.28

Residual Helmholtz energy is given by

$$\alpha_{CO_2}^r(\delta, \tau) = \sum_{i=1}^7 n_i \delta^{d_i} \tau^{t_i} + \sum_{i=8}^{34} n_i \delta^{d_i} \tau^{t_i} \exp(-\delta^{c_i}) \quad (29)$$

$$+ \sum_{i=35}^{39} n_i \delta^{d_i} \tau^{t_i} \exp(-\alpha_i(\delta - \epsilon_i)^2 - \beta_i(\tau - \gamma_i)^2) + \sum_{i=40}^{42} n_i \Delta^{b_i} \delta \Psi$$

with

$$\theta = (1 - \tau) + A_i [(\delta - 1)^2]^{1/(2\beta_i)} \quad (30)$$

$$\Delta = \theta^2 + B_i [(\delta - 1)^2]^{a_i} \quad (31)$$

$$\Psi = \exp(-C_i(\delta - 1)^2 - D_i(\tau - 1)^2) \quad (32)$$

The derivatives of $\alpha_{CO_2}^r$, θ , Δ and Ψ as required in the mixture model and values of the parameters n_i , d_i , t_i , c_i , α_i , β_i , γ_i , ϵ_i , a_i , b_i , A_i , B_i , C_i and D_i are given in [Appendix C](#).

2.4. Ideal Mixture of Real Gases Model

We will now discuss how the approach in ([Seiff et al., 1980](#)) can be followed using the equations of state in Helmholtz energy. To obtain the thermodynamic properties of ideal mixture of real gases (IMRG), the first step is to neglect the contribution of non-ideal interactions between the different components in the mixture model. This can be done by setting α^E to zero. The non-dimensionalized Helmholtz free energy of the IMRG can then be written as

$$\alpha^{IMRG}(\tilde{\rho}, T, \bar{x}) = \sum_{i=1}^n x_i [\alpha_i^o(\tilde{\rho}, T) + \ln x_i + \alpha_i^r(\delta_i, \tau_i)] \quad (33)$$

where $\delta_i = \tilde{\rho}/\tilde{\rho}_{c,i}$ is the reduced density and $\tau_i = T_{c,i}/T$ is the reduced temperature of component i . It is important to note that α_i^r is not a function of the mixture reduced density δ and mixture reduced temperature τ here. These reduced values depend on mixing rules which vary from one real gas mixture model to another as we have seen in the case of LJ-1999 and GERG-2008 models. The IMRG must not depend on the mixing rule being used. This approach is similar to that followed in ([STP-TS-012-1, 2012](#)). The thermodynamic properties of the IMRG can be obtained by using Gibbs-Dalton law which is valid for ideal mixtures

$$p = \sum_{i=1}^n x_i p_i; \quad \tilde{c}_v = \sum_{i=1}^n x_i \tilde{c}_{v,i}; \quad \tilde{c}_p = \sum_{i=1}^n x_i \tilde{c}_{p,i} \quad (34)$$

where p_i is the partial pressure of component i for $\tilde{\rho}$ and T which can be evaluated using [Eq.14](#). Similarly, $\tilde{c}_{v,i}$ is the partial specific isochoric heat capacity and $\tilde{c}_{p,i}$ is the partial isobaric specific heat capacity of component i which can be evaluated using [Eqs.15](#) and [16](#). Specifically, we have

$$p = \sum_{i=1}^n \tilde{\rho} R T x_i \left[1 + \delta_i \left(\frac{\partial \alpha_i^r}{\partial \delta_i} \right)_{\tau_i} \right] \quad (35)$$

$$\frac{\tilde{c}_v}{R} = - \sum_{i=1}^n x_i \tau_i^2 \left[\left(\frac{\partial^2 \alpha_i^o}{\partial \tau_i^2} \right) + \left(\frac{\partial^2 \alpha_i^r}{\partial \tau_i^2} \right)_{\delta_i} \right] \quad (36)$$

$$\frac{\tilde{c}_p}{R} = \frac{\tilde{c}_v}{R} + \sum_{i=1}^n x_i \frac{\left[1 + \delta_i \left(\frac{\partial \alpha_i^r}{\partial \delta_i} \right)_{\tau_i} - \delta_i \tau_i \left(\frac{\partial^2 \alpha_i^r}{\partial \delta_i \partial \tau_i} \right) \right]^2}{1 + 2\delta_i \left(\frac{\partial \alpha_i^r}{\partial \delta_i} \right)_{\tau_i} + \delta_i^2 \left(\frac{\partial^2 \alpha_i^r}{\partial \delta_i^2} \right)_{\tau_i}} \quad (37)$$

3. Density Solvers

As we have seen in the previous section, the independent variables for the mixture models in Helmholtz free energy are amount of substance density $\tilde{\rho}$ and temperature T . When pressure p and temperature are available to us, we need to solve for amount of substance density in Eqs.14 and 35. We use MATLAB’s inbuilt function `fzero` for root finding which uses a combination of bisection, secant, and inverse quadratic interpolation methods. The equations (Eqs.14 and 35) for which we need to obtain roots are highly nonlinear and many roots are possible. It is thus important to ascertain which root $\tilde{\rho}$ is physically meaningful. We follow the suggestions in (Gernert et al., 2014) to do this. MATLAB’s root finding solver `fzero` requires an initial estimate or interval for $\tilde{\rho}$ in which we believe the root lies in. This was generated using the ideal gas law or exploration of the range of Eqs.14 and 35 for different values of p and T . This could also be done through using an SRK equation of state as suggested in (Gernert et al., 2014).

4. Verification of the results with Available Experimental Results

We compare the approaches of pure CO_2 model (Staley, 1970), IMRG model (Seiff et al., 1980), LJ-1999 model (Lemmon and Jacobsen, 1999) and GERG-2008 model (Kunz and Wagner, 2012) against experimental data. Our main motivation is to show that the real gas mixture models perform better than the other approaches in predicting the thermodynamic properties of the real gas mixture $CO_2 - N_2$. Staley (1970) and Seiff et al. (1980) used the compilation of experimentally determined properties of CO_2 and N_2 found in Hilsenrath et al. (1955). To account for more recent experiments, we use the equations of state for CO_2 (Span and Wagner, 1996) and N_2 (Span et al., 2000). For comparison, the uncertainty in the isobaric specific heat capacity data of CO_2 tabulated in (Hilsenrath et al., 1955) is of the order of $\pm 2.0\%$ for $220\text{ K} \leq T \leq 600\text{ K}$ at atmospheric pressure. This is considering the experimental data available at that time which had low reliability. The uncertainty in c_p for CO_2 as obtained from the equation of state in Helmholtz energy (Span and Wagner, 1996) is of the order of $\pm 0.15\%$ at the same pressure when considered against more reliable experimental data. Considering N_2 , the uncertainty in c_p data obtained using the equation of state in Helmholtz energy (Span et al., 2000) is of the order of $\pm 0.3\%$ against that of $\pm 3.0\%$ uncertainty in c_p data of Hilsenrath et al. (1955) for $100\text{ K} \leq T \leq 700\text{ K}$ at atmospheric pressure.

For the comparing accuracy of the different models, we look at experiments that reported results for $CO_2 - N_2$ mixtures with $x_{CO_2} > 0.9$ as the main contention by the approach proposed by Seiff et al. (1980) was that non-ideal interactions between CO_2 and N_2 can be safely neglected for such mixtures. Table 5 summarizes the literature that was used.

Reference	Type of Expt. Data	Pressure Range (MPa)	Temperature Range (K)	x_{CO_2} (%)
Brugge et al. (1989)	$p\rho T$	0.21-6.63	300-320	90.92
Brugge et al. (1997)	$p\rho T$	1.03-69.09	285-450	90.92
Ely et al. (1989)	$p\rho T$	2.26-33.10	250-330	98.20
Mantovani et al. (2012)	$p\rho T$	1.00-20.00	303-383	90.21, 95.85
Bishnoi et al. (1972)	c_p	3.45-14.48	313-363	93.23

Table 5: Experimental Data for CO_2 Rich Mixtures of $CO_2 - N_2$

In Figures 1, 2, 3 and 4, we look at the relative deviations of density calculated using the different models against the experimental data. The results indicate that the GERG-2008 mixture

model is the most accurate for these temperature and pressure ranges followed by the LJ-1999 mixture model, then the IMRG model and lastly considering a pure CO_2 equation of state. In addition to comparing the trends of deviations, we can compare the percentage average absolute deviations in density (calculated over N data points) which is given by

$$AAD\%_{calc-exp} = \frac{1}{N} \sum_{i=1}^N 100 \frac{|\rho_{exp} - \rho_{calc}|}{\rho_{exp}} \quad (38)$$

where ρ_{exp} is the experimentally measured value of density and ρ_{calc} is that predicted by the mixture model. For example, the AAD% in density obtained from the different mixture models against the experimental data of (Brugge et al., 1989) are: (i) GERG-2008 – 0.0671, (ii) LJ-1999 – 0.2446, (iii) IMRG – 0.4842, and (iv) Pure CO_2 – 5.7316. The real gas mixture models are also able to give accurate values of density for the $CO_2 - N_2$ mixture in the supercritical region. Considering $x_{CO_2} = 0.9585$, the AAD% in density obtained from the different mixture models against the experimental data of (Mantovani et al., 2012) are: (i) GERG-2008 – 1.3592, (ii) LJ-1999 – 1.5421, (iii) IMRG – 2.6761, and (iv) Pure CO_2 – 9.8766.

This indicates that the real gas mixture models can be used with confidence in calculating accurate values of the thermodynamic properties for the $CO_2 - N_2$ mixture which exists in a supercritical state in the lower parts of the Venus atmosphere.

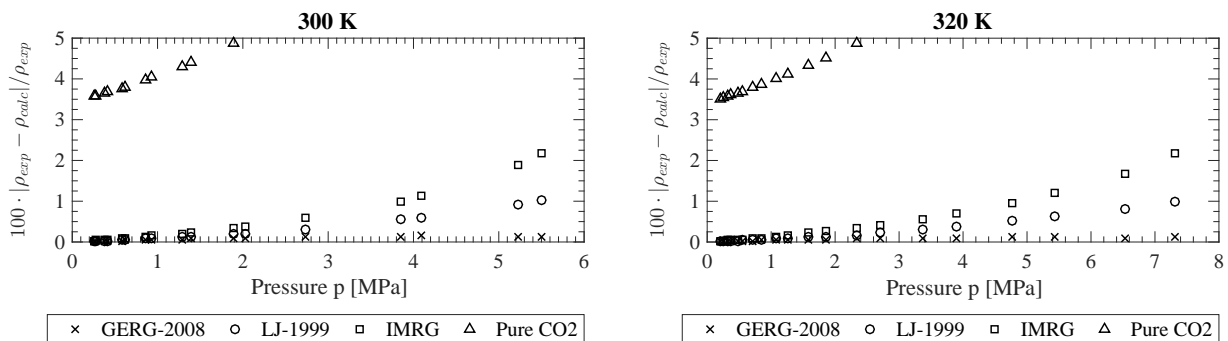


Figure 1: Deviations of density calculated using the different models from experimental data for $x_{CO_2} = 0.90921$ in (Brugge et al., 1989)

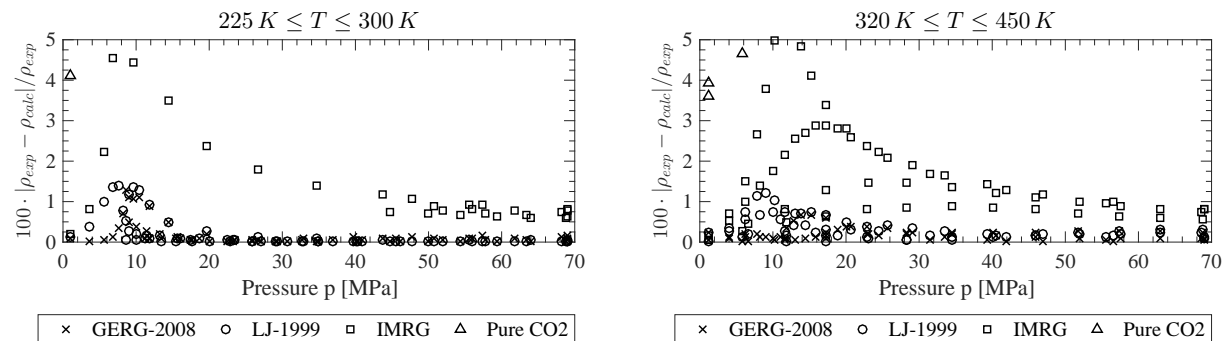


Figure 2: Deviations of density calculated using the different models from experimental data for $x_{CO_2} = 0.90921$ in (Brugge et al., 1997)

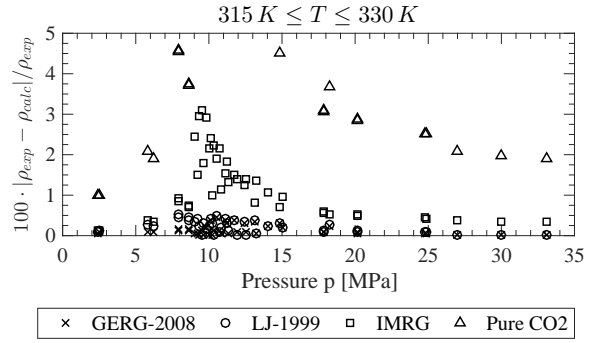
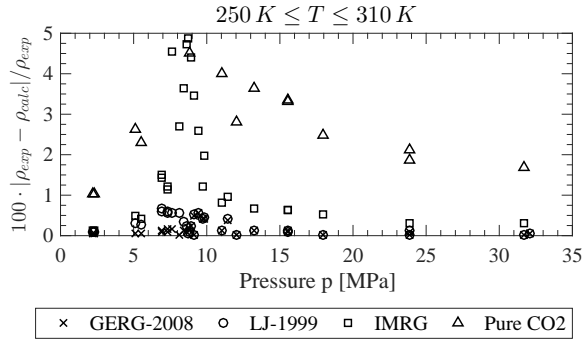
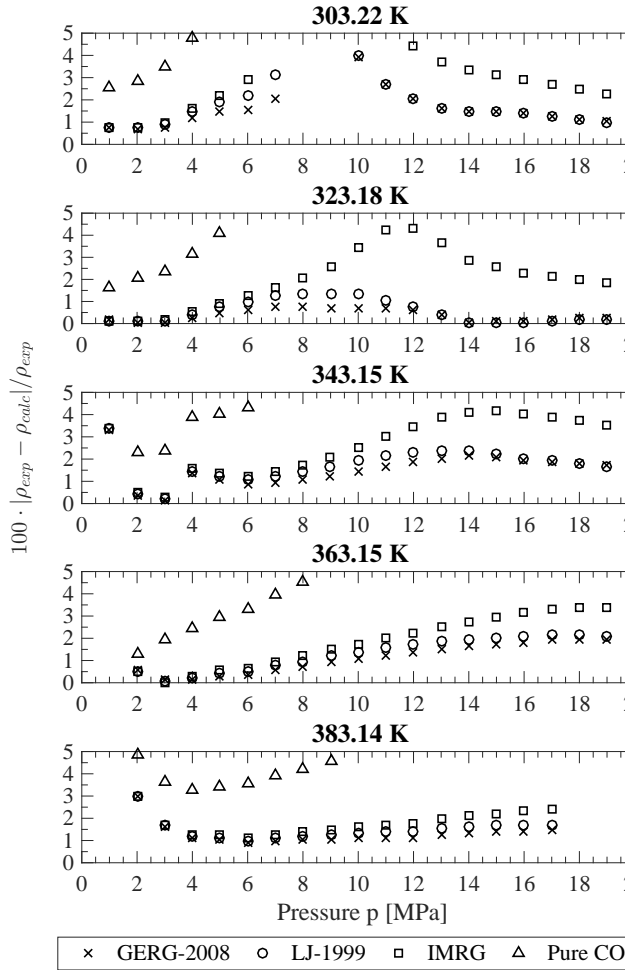
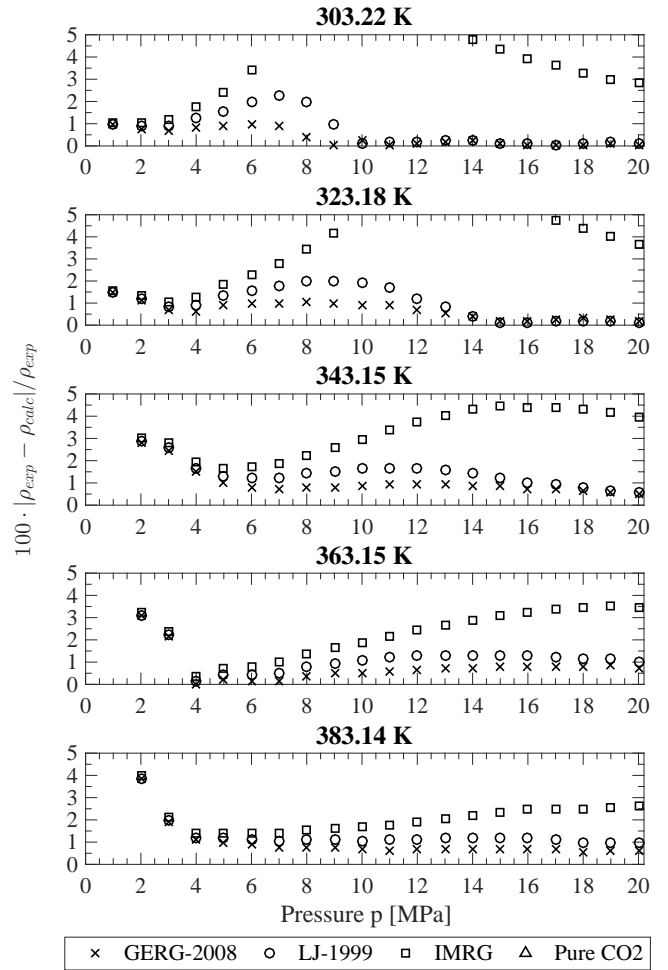


Figure 3: Deviations of density calculated using the different models from experimental data for $x_{CO_2} = 0.982$ in (Ely et al., 1989)



(a) $x_{CO_2} = 0.9585$



(b) $x_{CO_2} = 0.9021$

Figure 4: Deviations of density calculated using the different models from experimental data in (Mantovani et al., 2012)

Lastly, we look at the relative deviations of isobaric specific heat capacity calculated using the different models against the experimental data (Bishnoi et al., 1972). The trends in Figure 5 show

that the GERG-2008 and LJ-1999 mixture models are far more accurate than the IMRG model and the pure CO_2 equation of state at predicting values of c_p . The AAD% in c_p over the real gas mixture models against the experimental data of (Bishnoi et al., 1972) are (i) GERG-2008 – 1.7083, and (ii) LJ-1999 – 2.1151.

Through the comparison of the different mixture models against experimental data, we have seen that it is imperative to include the non-ideal interactions of CO_2 and N_2 in the mixture when calculating the thermodynamic properties of the mixture. Moreover, this served as a verification of our implementation of the different real gas mixture models. The trends of deviations in ρ and c_p obtained here closely match with those in (Gernert, 2013) for the GERG-2008 model and (Lemmon, 1996) for the

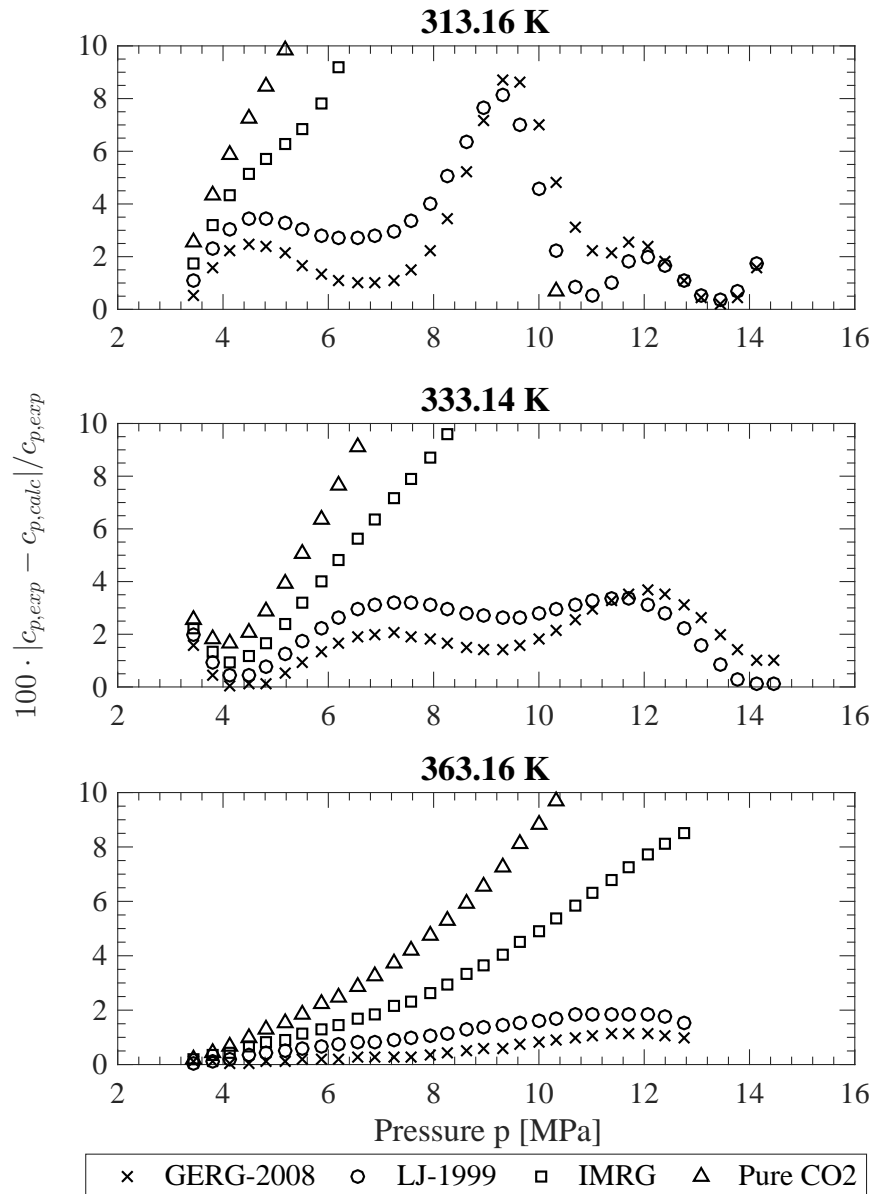


Figure 5: Deviations of isobaric heat capacities calculated using the different models from experimental data for $x_{CO_2} = 0.9323$ in (Bishnoi et al., 1972)

5. Adiabatic Lapse Rate

5.1. LJ-1999, GERG-2008 and Pure CO₂ Models

Our starting point for calculating adiabatic lapse rate is Eq.1

$$\Gamma = -\frac{T \left(\frac{\partial p}{\partial T} \right)_\rho}{\rho \left(\frac{\partial p}{\partial \rho} \right)_T} \left(\frac{g}{c_p} \right) \quad (39)$$

Isobaric heat capacity c_p can be computed using Eq.16. We further note that from Eq.14 and using the definitions of reducing functions, the different partial derivatives of pressure can be computed from

$$\left(\frac{\partial p}{\partial T} \right)_\rho = \tilde{\rho} R (1 + \delta \alpha_\delta^r - \delta \tau \alpha_{\delta\tau}^r) \quad (40)$$

$$\left(\frac{\partial p}{\partial \rho} \right)_T = \frac{RT}{M} (1 + 2\delta \alpha_\delta^r + \delta^2 \alpha_{\delta\delta}^r) \quad (41)$$

The adiabatic lapse rate can then be computed using

$$\Gamma = -\frac{(1 + \delta \alpha_\delta^r - \delta \tau \alpha_{\delta\tau}^r)}{(1 + 2\delta \alpha_\delta^r + \delta^2 \alpha_{\delta\delta}^r)} \left(\frac{g}{c_p} \right) \quad (42)$$

In the above expression, acceleration due to gravity was assumed to change only with altitude z as $g = g_o \frac{R_o^2}{(R_o+z)^2}$ where $g_o = 8.869m/s^2$ and the radius of the planet of Venus R_o was considered to be 6052 km.

The atmospheric conditions of Venus are recorded in terms of pressure p and temperature T . As a part of calculating Γ , density ρ needs to be determined. We follow the discussion in Sec.3 and additionally consider the initial estimate of density from interpolated values of density reported in (Moroz, 1981) for altitude range of 0 – 100km.

5.2. IMRG Model

We follow the same approach as discussed in Seiff et al. (1980) to calculate the adiabatic lapse rate for the ideal mixture of real gases model (IMRG). The only difference is that the thermodynamic properties of the IMRG model are determined from equations of state in Helmholtz free energy as was discussed in Sec. 2.4. The expression in Eq.2 can be calculated using

$$\Gamma = b \left(\frac{g}{c_p} \right) \quad (43)$$

where c_p is calculated using Eq.37 and $b = -aT$ (with a as defined in Eq.3). For the IMRG model, b can be calculated as

$$b = -\sum_i x_i \left[\frac{T}{\rho} \left(\frac{\partial \rho}{\partial T} \right)_p \right]_i \quad (44)$$

$$= -\sum_i x_i \left[\frac{T}{\rho} \frac{\left(\frac{\partial p}{\partial T} \right)_\rho}{\left(\frac{\partial p}{\partial \rho} \right)_T} \right]_i \quad (45)$$

The expressions for the partial derivatives of p for component i can be written in a similar fashion to those in Eqs.40 and 41. The expression for adiabatic lapse rate for the IMRG model then becomes

$$\Gamma = - \left(\sum_i x_i \left[\frac{(1 + \delta_i \alpha_{\delta_i}^r - \delta_i \tau_i \alpha_{\delta_i \tau_i}^r)}{(1 + 2\delta_i \alpha_{\delta_i}^r + \delta_i^2 \alpha_{\delta_i \delta_i}^r)} \right] \right) \left(\frac{g}{c_p} \right) \quad (46)$$

where α^r is different for each component i .

6. Results and Discussion

Oyama et al. (1980) reported a vertical gradient of N_2 between 22 and 52km altitudes. However, for the sake of comparison, we consider the Venus atmosphere to be composed of a real gas binary mixture of $CO_2 - N_2$ in the constant volume mixing ratio of 96.5 : 3.5 (Von Zahn et al., 1983). Additionally, we can assume within experimental uncertainty that the atmosphere can be considered to be composed of a real gas binary mixture of $CO_2 - N_2$ in a ratio of 96.5 : 3.5 by mole fraction. Thus, we neglect any vertical variation in the composition.

An atmospheric model of Venus was created in (Seiff et al., 1985) using the measurements obtained from the four Pioneer Venus probes. Details of the profiles measured by these probes can be found in (Seiff et al., 1980). The vertical profile of the adiabatic lapse rate for this atmospheric model was computed with the different mixture models which we have discussed using Eqs. 42 and 46. The results for the GERG-2008 mixture model which was shown to be the most accurate mixture model against experimental data in Section 4 are shown in Figure 6(b). The adiabatic lapse rate decreases with decreasing pressure and temperature from the surface by almost 1.5 K/km between surface and 50 km and increases by the same amount in the next 20 km between 50-70 km. Figure 7 shows the difference between Seiff et al. (1985) adiabatic lapse rate computed for ideal mixture of $CO_2 - N_2$ (i.e. ignoring the real gas $CO_2 - N_2$ interactions) and adiabatic lapse rate computed from the GERG-2008 model. The differences in the calculations are as high as 0.02 K/km around 20 km. This is high enough to characterize layers in the atmosphere close to neutrally stable, which were thought to be initially stable as now unstable. This shows the importance of taking non-ideal interactions in the real gas mixture into account and using more recent experimental data of CO_2 and N_2 represented by their equations of state.

VeGa 2 temperature profile (Linkin et al., 1987) is the only one that provides measurements below 12 km and the adiabatic lapse rates corresponding to this profile computed from the GERG-2008 model is shown in Figure 6(b). The corresponding static stability profiles are shown in Figure 8 which was calculated using

$$\Delta\Gamma = \left(\frac{dT}{dz} \right)_{meas} - \left(\frac{dT}{dz} \right)_{ad} = \left(\frac{dT}{dz} \right)_{meas} + \Gamma \quad (47)$$

where $\left(\frac{dT}{dz} \right)_{meas}$ is the gradient of the measured temperature with respect to altitude. This was computed using a second order centered scheme from the available temperature measurements. The nonlinear Savitzky-Golay filter was applied to the static stability profile computed for (Linkin et al., 1987) with a span of 11 points to remove spurious oscillations. Two superadiabatic layers are seen - one near the surface at about 4 km and another at about 17 km. A layer of near neutral stability or even slightly unstable layer is also seen in the VeGa 2 profile between 50-54 km. In the static stability profile for Seiff et al. (1985), the atmosphere is stable near the surface. This difference

between the static stability plots in Figure 8 can be explained by looking at the difference in adiabatic lapse rates obtained in Figure 6(b) near the surface for altitudes of 0 – 15km.

For obtaining the adiabatic lapse rate and static stability for the higher altitudes in the Venus atmosphere, we use the pT profiles (Figure 9) obtained from radio occultation studies with the Magellan spacecraft (Steffes et al., 1994; Jenkins et al., 1994). The temperature profile used for the calculation of adiabatic lapse rate and static stability are from orbit 3212 of the spacecraft and is shown in Figure 9. The results obtained for adiabatic lapse rate is shown in Figure 10(a) and for static stability is shown in Figure 10(b). The vertical profile of static stability obtained using the GERG-2008 mixture model is similar to the one obtained in (Hinson and Jenkins, 1995). Differences are due to the fact that (Hinson and Jenkins, 1995) used values of Γ from (Seiff et al., 1980).

From the infrared spectrometry data onboard Venera-15 (Zasova et al., 2006), it was observed that there are spatial and temporal variations in the upper atmosphere. To fully understand the convective stability in the Venus atmosphere, we take these into consideration when calculating adiabatic lapse rate and static stability. Figure 11 shows the profiles of adiabatic lapse rate and static stability for latitudes $\phi < 35^\circ$ and for various solar longitudes. Not only are there clear variations in the magnitude of static stability from 75 – 100 km, we also observe that the atmosphere is unstable from 50 – 52 km for solar longitude $L_S = 270^\circ - 310^\circ$ but stable otherwise. This indicates the importance of considering the variation in adiabatic lapse rate with both altitude and latitude.

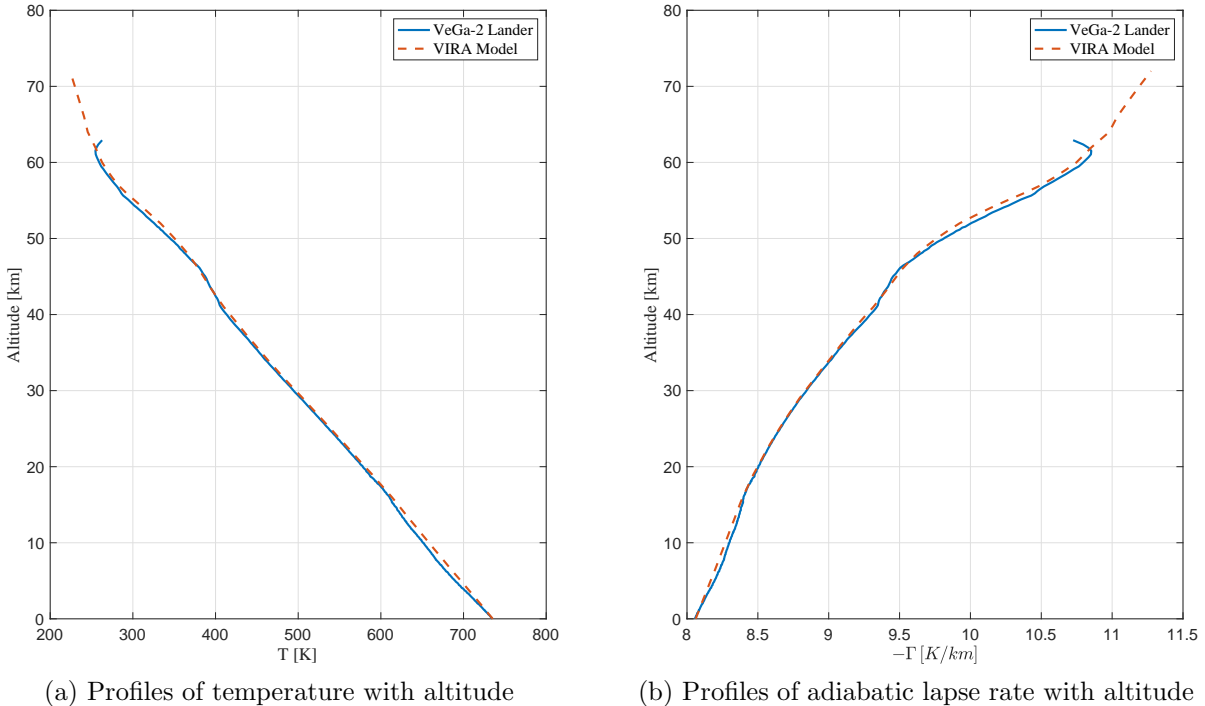


Figure 6: Comparison of profiles of temperature and adiabatic lapse rate computed using the GERG-2008 mixture model for the VeGa-2 Lander (Linkin et al., 1987) and the VIRA model (Seiff et al., 1985) constructed from the four Pioneer Venus probes’ data (Seiff et al., 1980)

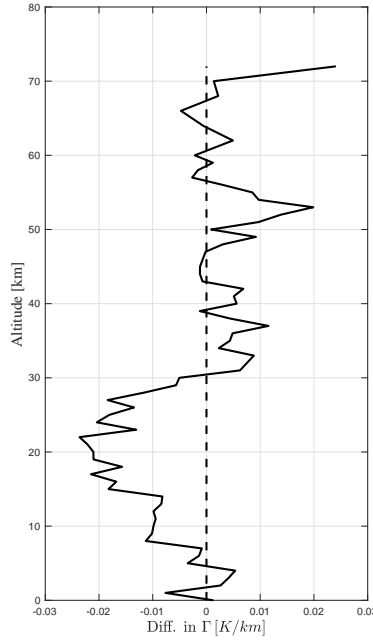


Figure 7: $\Gamma^{\text{Seiff1980}} - \Gamma^{\text{GERG2008}}$: Difference in adiabatic lapse rates computed for the VIRA model using the GERG-2008 model and that calculated in (Seiff et al., 1985)

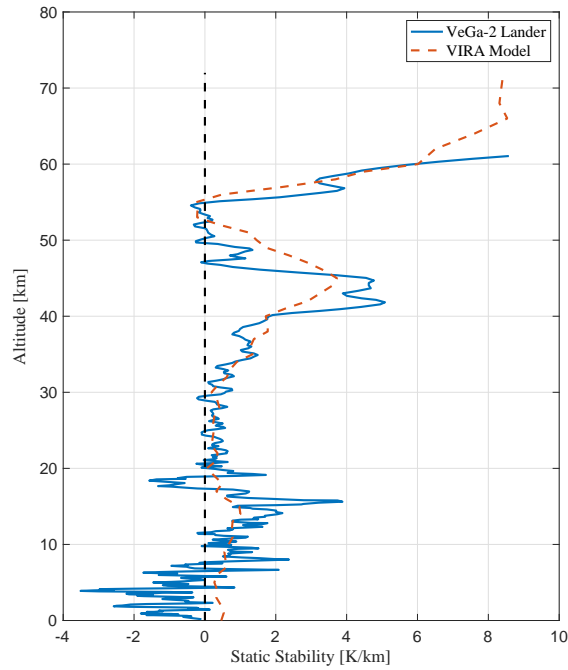


Figure 8: Comparison of profiles of static stability with altitude in the Venus atmosphere computed using the GERG-2008 mixture model considering the profiles measured by the VeGa-2 Lander (Linkin et al., 1987) and the VIRA model (Seiff et al., 1985) constructed from the four Pioneer Venus probes' data (Seiff et al., 1980)

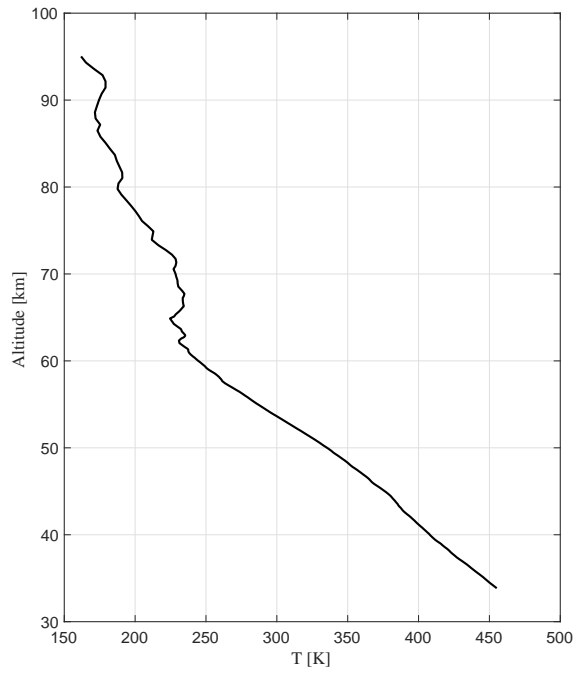
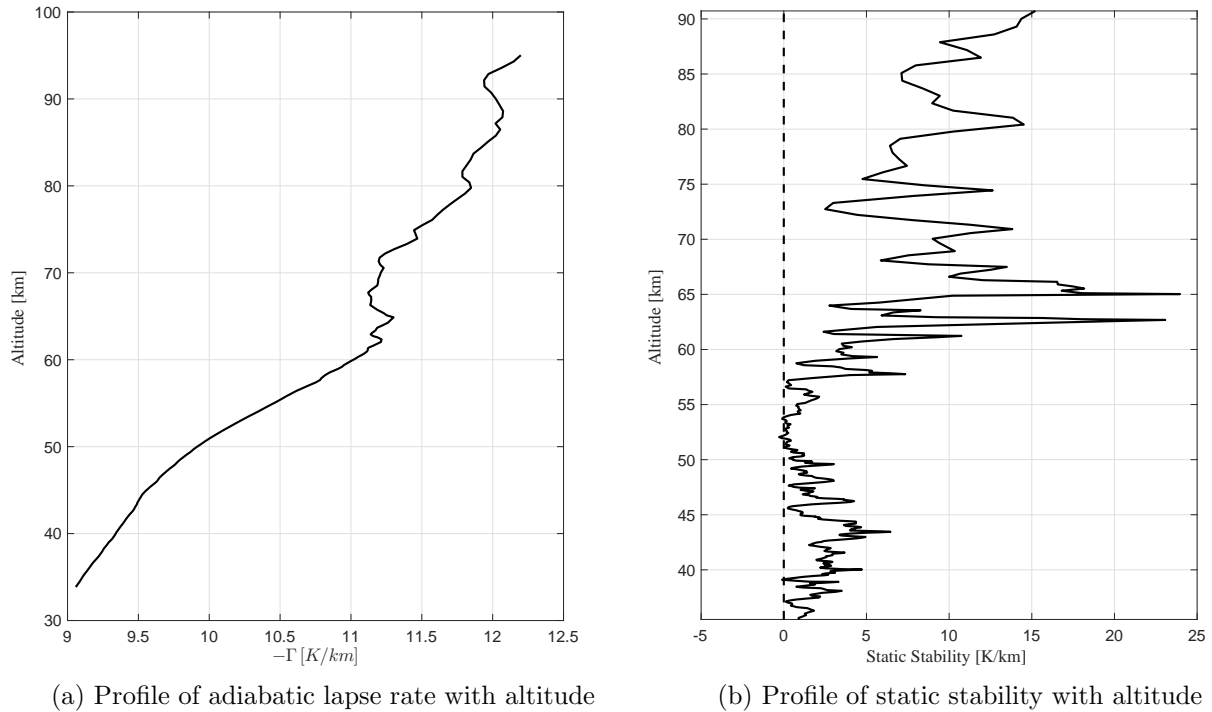


Figure 9: Profile of temperature with altitude of orbit 3212 of the Magellan spacecraft (Steffes et al., 1994; Jenkins et al., 1994)



(a) Profile of adiabatic lapse rate with altitude

(b) Profile of static stability with altitude

Figure 10: Profiles of adiabatic lapse rate and static stability with altitude in the Venus atmosphere considering the profile of orbit 3212 of the Magellan spacecraft (Steffes et al., 1994; Jenkins et al., 1994) calculated using the GERG-2008 mixture model

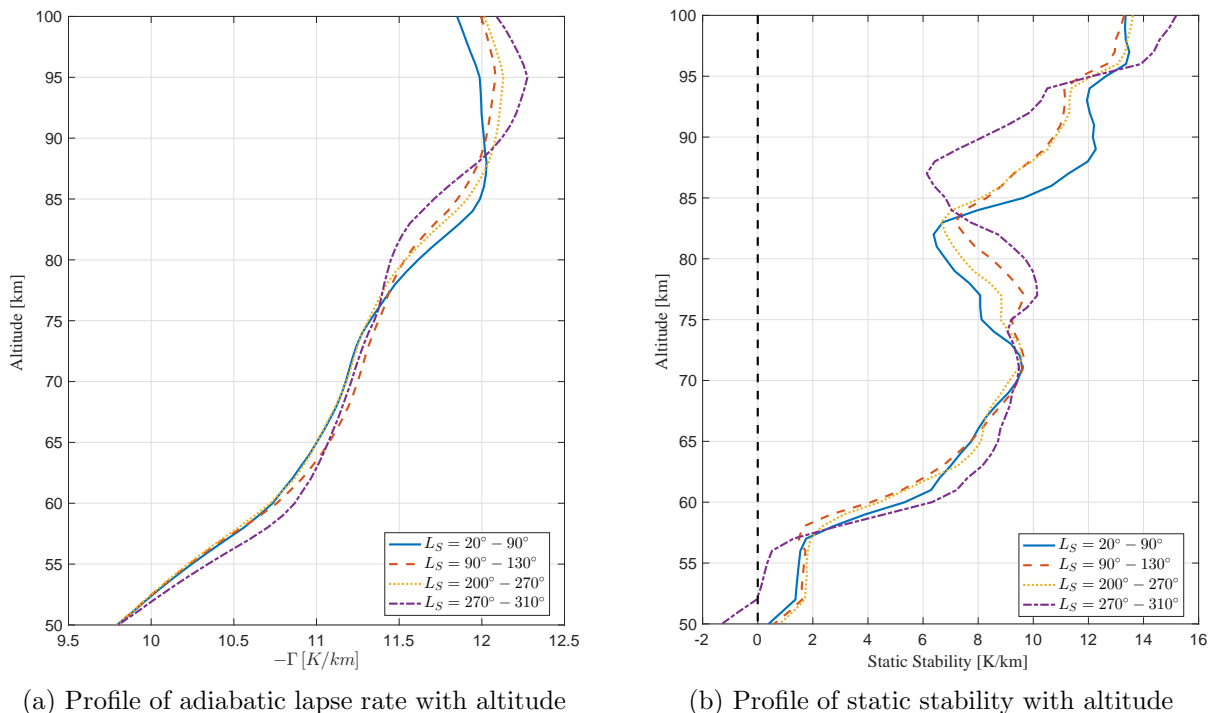


Figure 11: Profiles of adiabatic lapse rate and static stability with altitude as a function of solar longitude in the upper atmosphere of Venus atmosphere calculated using the GERG-2008 mixture model, considering the Venera 15 Fourier Spectrometer data (Zasova et al., 2006)

7. Conclusion and Future Work

We have calculated more accurate values of the adiabatic lapse rate for a mixture of 96.5% carbon dioxide and 3.5% nitrogen using the GERG-2008 mixture model for the temperature and pressure conditions found in the Venus atmosphere. We were able to account for the difference in adiabatic lapse rate values due to non-ideal interactions between CO_2 and N_2 . Near the altitudes of 20km, the magnitude of our value is about 0.02K/km lower than the approximate value calculated by Seiff et al. (1980). We showed the importance of considering spatial variations in adiabatic lapse rate with latitude and altitude as well as temporal variations. These calculations can also be performed considering the Venus atmosphere composition to vary with altitude to reflect the measured differences in the composition. It was shown in (Oyama et al., 1980) that the abundance of nitrogen in the atmosphere can be as high as 4.6 v% at 51.6km and more recent studies (Peplowski and Lawrence, 2016) have reported higher values of 5.38 v% at 60 – 70km. Further, considering the gradient in molecular weight with altitude will alter all available profiles of $T(p)$ for occultation and entry probe measurements, and $T(z)$ for non occultation results. Moreover, this approach can be applied to other planets or moons such as Saturn’s largest moon Titan which has an atmosphere composed of mainly nitrogen and methane.

Acknowledgments

Arkopal Dutt acknowledges support from the Indo US Science and Technology Foundation for the S.N. Bose Scholarship at University of Wisconsin-Madison. Funding from NASA Grant NNX09AE85G for completion of this work is acknowledged.

Appendix A. Derivation of Real Gas Adiabatic Lapse Rate

Here, we outline a derivation of the real gas adiabatic lapse rate along the lines of [Staley \(1970\)](#) and show it is applicable to any planetary atmosphere with altitude varying real gas mixture composition. The system in consideration is a parcel of air composed of m real gas components at altitude z . There are n_i moles of component gas i . This parcel of air is engaged in the adiabatic process of rising in the atmosphere. The first law of thermodynamics gives us the following relationship between the internal energy U , heat Q and work done W on the system

$$dU = \delta Q - \delta W + \sum_i \mu_i dn_i \quad (\text{A.1})$$

where μ_i is the chemical potential of the i th component gas of the system and dn_i is the change in number of moles of that particular component. Considering that the parcel of air has a constant composition while rising,

$$dU = \delta Q - \delta W \quad (\text{A.2})$$

Assuming specific internal energy u as a function of temperature T , specific volume v and composition we have

$$du = \left(\frac{\partial u}{\partial T} \right)_{v, \sum n_i} dT + \left(\frac{\partial u}{\partial v} \right)_{T, \sum n_i} dv + \sum_j \left(\frac{\partial u}{\partial n_j} \right)_{T, v, \sum_{i \neq j} n_i} dn_j \quad (\text{A.3})$$

where the subscript $\sum n_i$ denotes that the mole numbers of all the component gases is held constant for the corresponding partial derivative and $\sum_{j \neq i} n_j$ denotes that the mole numbers of all component gases but j th component is held constant. Noting that the composition of the air parcel does not change while rising, the above equation is simplified to

$$du = c_v dT + \left(\frac{\partial u}{\partial v} \right)_T dv \quad (\text{A.4})$$

where c_v is the isochoric specific heat capacity. Using the Maxwell's relation of

$$\left(\frac{\partial u}{\partial v} \right)_T = T \left(\frac{\partial p}{\partial T} \right)_v - p \quad (\text{A.5})$$

where p is pressure in the parcel, we obtain from substituting in [Eq.A.2](#):

$$dq = c_v dT + T \left(\frac{\partial p}{\partial T} \right)_v dv \quad (\text{A.6})$$

If we were to introduce an equation of state explicit in pressure $p = p(v, T, n_i)$, we would then have

$$dp = \left(\frac{\partial p}{\partial T} \right)_{v, \sum n_i} dT + \left(\frac{\partial p}{\partial v} \right)_{T, \sum n_i} dv + \sum_j \left(\frac{\partial p}{\partial n_j} \right)_{T, v, \sum_{i \neq j} n_i} dn_j \quad (\text{A.7})$$

which reduces to

$$dp = \left(\frac{\partial p}{\partial T} \right)_v dT + \left(\frac{\partial p}{\partial v} \right)_T dv \quad (\text{A.8})$$

as the parcel maintains constant composition while rising. Writing it explicitly in terms of volume differential, we have

$$dv = \frac{dp - \left(\frac{\partial p}{\partial T}\right)_v dT}{\left(\frac{\partial p}{\partial v}\right)_T} \quad (\text{A.9})$$

Substituting above in Eq.A.6, we get

$$dq = \left[c_v - \frac{T \left(\frac{\partial p}{\partial T}\right)_v^2}{\left(\frac{\partial p}{\partial v}\right)_T} \right] dT + T \frac{\left(\frac{\partial p}{\partial T}\right)_v}{\left(\frac{\partial p}{\partial v}\right)_T} dp \quad (\text{A.10})$$

$$dq = c_p dT + T \frac{\left(\frac{\partial p}{\partial T}\right)_v}{\left(\frac{\partial p}{\partial v}\right)_T} dp \quad (\text{A.11})$$

where c_p is the isobaric specific heat capacity of the multi-component real gas mixture that makes up the parcel of air. Assuming adiabatic condition and using the hydrostatic equation $dp = -\rho g dz$ where $\rho (= 1/v)$ is the density of the air parcel, the following expression for adiabatic lapse rate Γ is obtained.

$$\Gamma = -\frac{dT}{dz} = -T \rho \frac{\left(\frac{\partial p}{\partial T}\right)_v}{\left(\frac{\partial p}{\partial v}\right)_T} \left(\frac{g}{c_p}\right) = \frac{T}{\rho} \frac{\left(\frac{\partial p}{\partial T}\right)_\rho}{\left(\frac{\partial p}{\partial \rho}\right)_T} \left(\frac{g}{c_p}\right) \quad (\text{A.12})$$

Appendix B. Equation of State for N_2

Derivatives required for the evaluation of thermodynamic properties are given by

$$\left(\frac{\partial^2 \alpha_{N_2}^0}{\partial \tau^2}\right)_\delta = -a_{1\tau} \tau^{-2} + 2a_{4\tau} \tau^{-3} + 6a_{5\tau} \tau^{-4} + 12a_{6\tau} \tau^{-5} - a_{7a_8} \frac{\exp(a_8 \tau)}{[\exp(a_8 \tau) - 1]^2} \quad (\text{B.1})$$

$$\begin{aligned} \left(\frac{\partial \alpha_{N_2}^r}{\partial \delta}\right)_\tau &= \sum_{k=1}^6 i_k N_k \delta^{i_k-1} \tau^{j_k} + \sum_{k=7}^{32} N_k \delta^{i_k-1} \tau^{j_k} \exp(-\delta^{l_k}) (i_k - l_k \delta^{l_k}) \\ &+ \sum_{k=33}^{36} N_k \delta^{i_k-1} \tau^{j_k} \exp(-\phi_k (\delta - 1)^2 - \beta_k (\tau - \gamma_k)^2) [i_k - 2\delta \phi_k (\delta - 1)] \end{aligned} \quad (\text{B.2})$$

$$\begin{aligned} \left(\frac{\partial^2 \alpha_{N_2}^r}{\partial \delta^2}\right)_\tau &= \sum_{k=1}^6 i_k (i_k - 1) N_k \delta^{i_k-2} \tau^{j_k} + \sum_{k=7}^{32} N_k \delta^{i_k-2} \tau^{j_k} \exp(-\delta^{l_k}) [(i_k - l_k \delta^{l_k})(i_k - 1 - l_k \delta^{l_k}) - l_k^2 \delta^{l_k}] \\ &+ \sum_{k=33}^{36} N_k \delta^{i_k-2} \tau^{j_k} \exp(-\phi_k (\delta - 1)^2 - \beta_k (\tau - \gamma_k)^2) \{ [i_k - 2\phi_k \delta (\delta - 1)]^2 - i_k - 2\delta^2 \phi_k \} \end{aligned} \quad (\text{B.3})$$

k	N_k	i_k	j_k	l_k	k	N_k	i_k	j_k	l_k
1	0.924803575275	1	0.250	0	19	-0.043576233605	1	4.000	2
2	-0.492448489428	1	0.875	0	20	-0.072317488932	2	6.000	2
3	0.661883336938	2	0.500	0	21	0.038964431527	3	6.000	2
4	-1.929026492010	2	0.875	0	22	-0.021220136391	4	3.000	2
5	-0.062246930963	3	0.375	0	23	0.004088229815	5	3.000	2
6	0.349943957581	3	0.750	0	24	-0.000055199002	8	6.000	2
7	0.564857472498	1	0.500	1	25	-0.046201671648	4	16.000	3
8	-1.617200059870	1	0.750	1	26	-0.003003117160	5	11.000	3
9	-0.481395031883	1	2.000	1	27	0.036882589121	5	15.000	3
10	0.421150636384	3	1.250	1	28	-0.002558568462	8	12.000	3
11	-0.016196223083	3	3.500	1	29	0.008969152646	3	12.000	4
12	0.172100994165	4	1.000	1	10	-0.004415133704	5	7.000	4
13	0.007354489249	6	0.500	1	31	0.001337229249	6	4.000	4
14	0.016807730548	6	3.000	1	32	0.000264832492	9	16.000	4
15	-0.001076266642	7	0.000	1	33	19.668819401500	1	0.000	2
16	-0.013731808851	7	2.750	1	34	-20.911560073000	1	1.000	2
17	0.000635466900	8	0.750	1	35	0.016778830699	3	2.000	2
18	0.003044322794	8	2.500	1	36	2627.675662740000	2	3.000	2

k	ϕ_k	β_k	γ_k
33	20	325	1.16
34	20	325	1.16
35	15	300	1.13
36	25	275	1.25

Table B.6: Parameters as in Eq.27

$$\begin{aligned}
\left(\frac{\partial^2 \alpha_{N_2}^\tau}{\partial \delta \partial \tau}\right) &= \sum_{k=1}^6 i_k j_k N_k \delta^{i_k-1} \tau^{j_k-1} + \sum_{k=7}^{32} j_k N_k \delta^{i_k-1} \tau^{j_k-1} \exp(-\delta^{l_k}) (i_k - l_k \delta^{l_k}) \\
&+ \sum_{k=33}^{36} N_k \delta^{i_k-1} \tau^{j_k-1} \exp(-\phi_k(\delta-1)^2 - \beta_k(\tau-\gamma_k)^2) [i_k - 2\delta\phi_k(\delta-1)][j_k - 2\tau\beta_k(\tau-\gamma_k)]
\end{aligned} \tag{B.4}$$

$$\begin{aligned}
\left(\frac{\partial^2 \alpha_{N_2}^\tau}{\partial \tau^2}\right)_\delta &= \sum_{k=1}^6 j_k(j_k-1) N_k \delta^{i_k} \tau^{j_k-2} + \sum_{k=7}^{32} j_k(j_k-1) N_k \delta^{i_k} \tau^{j_k-2} \exp(-\delta^{l_k}) \\
&+ \sum_{k=33}^{36} N_k \delta^{i_k} \tau^{j_k-2} \exp(-\phi_k(\delta-1)^2 - \beta_k(\tau-\gamma_k)^2) \{[j_k - 2\beta_k\tau(\tau-\gamma_k)]^2 - j_k - 2\tau^2\beta_k\}
\end{aligned} \tag{B.5}$$

i	n_i	d_i	t_i	c_i	i	n_i	d_i	t_i	c_i
1	0.38856823203161	1	0.000		18	-0.01677587970043	1	6.000	2
2	2.93854759427400	1	0.750		19	-0.11960736637987	4	3.000	2
3	-5.58671885349340	1	1.000		20	-0.04561936250878	4	6.000	2
4	-0.76753199592477	1	2.000		21	0.03561278927035	4	8.000	2
5	0.31729005580416	2	0.750		22	-0.00744277271321	7	6.000	2
6	0.54803315897767	2	2.000		23	-0.00173957049024	8	0.000	2
7	0.12279411220335	3	0.750		24	-0.02181012128953	2	7.000	3
8	2.16589615432200	1	1.500	1	25	0.02433216655924	3	12.000	3
9	1.58417351097240	2	1.500	1	26	-0.03744013342346	3	16.000	3
10	-0.23132705405503	4	2.500	1	27	0.14338715756878	5	22.000	4
11	0.05811691643144	5	0.000	1	28	-0.13491969083286	5	24.000	4
12	-0.55369137205382	5	1.500	1	29	-0.02315122505348	6	16.000	4
13	0.48946615909422	5	2.000	1	30	0.01236312549290	7	24.000	4
14	-0.02427573984350	6	0.000	1	31	0.00210583219729	8	8.000	4
15	0.06249479050168	6	1.000	1	32	-0.00033958519026	10	2.000	4
16	-0.12175860225246	6	2.000	1	33	0.00559936517716	4	28.000	5
17	-0.37055685270086	1	3.000	2	34	-0.00030335118056	8	14.000	6

i	n_i	d_i	t_i	α_i	β_i	γ_i	ϵ_i
35	-213.65488688320000	2	1.000	25	325	1.16	1
36	26641.56914927200000	2	0.000	25	300	1.19	1
37	-24027.21220455700000	2	1.000	25	300	1.19	1
38	-283.41603423999000	3	3.000	15	275	1.25	1
39	212.47284400179000	3	3.000	20	275	1.22	1

i	n_i	a_i	b_i	β_i	A_i	B_i	C_i	D_i
40	-0.66642276540751	3.5	0.875	0.3	0.7	0.3	10	275
41	0.72608632349897	3.5	0.925	0.3	0.7	0.3	10	275
42	0.05506866861284	3	0.875	0.3	0.7	1	12.5	275

Table C.7: Parameters as in Eq.29

Appendix C. Equation of State for CO_2

Derivatives as required are given by

$$\begin{aligned}
\left(\frac{\partial \alpha_{CO_2}^r}{\partial \delta}\right)_\tau &= \sum_{i=1}^7 n_i d_i \delta^{d_i-1} \tau^{t_i} + \sum_{i=8}^{34} n_i \exp(-\delta^{c_i}) [\delta^{d_i-1} \tau^{t_i} (d_i - c_i \delta^{c_i})] \\
&+ \sum_{i=35}^{39} n_i \delta^{d_i} \tau^{t_i} \exp(-\alpha_i (\delta - \epsilon_i)^2 - \beta_i (\tau - \gamma_i)^2) \left[\frac{d_i}{\delta} - 2\alpha_i (\delta - \epsilon_i) \right] \\
&+ \sum_{i=40}^{42} n_i \left[\Delta^{b_i} \left(\Psi + \delta \frac{\partial \Psi}{\partial \delta} \right) + \frac{\partial \Delta^{b_i}}{\partial \delta} \delta \Psi \right]
\end{aligned} \tag{C.1}$$

$$\begin{aligned}
\left(\frac{\partial^2 \alpha_{CO_2}^r}{\partial \delta^2}\right)_\tau &= \sum_{i=1}^7 n_i d_i (d_i - 1) \delta^{d_i - 2} \tau^{t_i} + \sum_{i=8}^{34} n_i \exp(-\delta^{c_i}) [\delta^{d_i - 2} \tau^{t_i} ((d_i - c_i \delta^{c_i})(d_i - 1 - c_i \delta^{c_i}) - c_i^2 \delta^{c_i}) \\
&\quad + \sum_{i=35}^{39} n_i \tau^{t_i} \exp(-\alpha_i (\delta - \epsilon_i)^2 - \beta_i (\tau - \gamma_i)^2) \\
&\quad \times [-2\alpha_i \delta^{d_i} + 4\alpha_i^2 \delta^{d_i - 1} (\delta - \epsilon_i)^2 - 4d_i \alpha_i \delta^{d_i - 1} (\delta - \epsilon_i) + d_i (d_i - 1) \delta^{d_i - 2}] \\
&\quad + \sum_{i=40}^{42} n_i \left[\Delta^{b_i} \left(2 \frac{\partial \Psi}{\partial \delta} + \delta \frac{\partial^2 \Psi}{\partial \delta^2} \right) + 2 \frac{\partial \Delta^{b_i}}{\partial \delta} \left(\Psi + \delta \frac{\partial \Psi}{\partial \delta} \right) + \frac{\partial^2 \Delta^{b_i}}{\partial \delta^2} \delta \Psi \right]
\end{aligned} \tag{C.2}$$

$$\begin{aligned}
\left(\frac{\partial^2 \alpha_{CO_2}^r}{\partial \delta \partial \tau}\right) &= \sum_{i=1}^7 n_i d_i t_i \delta^{d_i - 1} \tau^{t_i - 1} + \sum_{i=8}^{34} n_i \exp(-\delta^{c_i}) \delta^{d_i - 1} t_i \tau^{t_i - 1} (d_i - c_i \delta^{c_i}) \\
&\quad + \sum_{i=35}^{39} n_i \delta^{d_i} \tau^{t_i} \exp(-\alpha_i (\delta - \epsilon_i)^2 - \beta_i (\tau - \gamma_i)^2) \left[\frac{d_i}{\delta} - 2\alpha_i (\delta - \epsilon_i) \right] \left[\frac{t_i}{\tau} - 2\beta_i (\tau - \gamma_i) \right] \\
&\quad + \sum_{i=40}^{42} n_i \left[\Delta^{b_i} \left(\frac{\partial \Psi}{\partial \tau} + \delta \frac{\partial^2 \Psi}{\partial \delta \partial \tau} \right) + \delta \frac{\partial \Delta^{b_i}}{\partial \delta} \frac{\partial \Psi}{\partial \tau} + \frac{\partial \Delta^{b_i}}{\partial \tau} \left(\Psi + \delta \frac{\partial \Psi}{\partial \delta} \right) + \frac{\partial^2 \Delta^{b_i}}{\partial \delta \partial \tau} \delta \Psi \right]
\end{aligned} \tag{C.3}$$

$$\begin{aligned}
\left(\frac{\partial^2 \alpha_{CO_2}^r}{\partial \tau^2}\right)_\delta &= \sum_{i=1}^7 n_i t_i (t_i - 1) \delta^{d_i} \tau^{t_i - 1} + \sum_{i=8}^{34} n_i t_i (t_i - 1) \delta^{d_i} \tau^{t_i - 2} \exp(-\delta^{c_i}) \\
&\quad + \sum_{i=35}^{39} n_i \delta^{d_i} \tau^{t_i} \exp(-\alpha_i (\delta - \epsilon_i)^2 - \beta_i (\tau - \gamma_i)^2) \left[\left(\frac{t_i}{\tau} - 2\beta_i (\tau - \gamma_i) \right)^2 - \frac{t_i}{\tau^2} - 2\beta_i \right] \\
&\quad + \sum_{i=40}^{42} n_i \delta \left[\frac{\partial^2 \Delta^{b_i}}{\partial \tau^2} \Psi + 2 \frac{\partial \Delta^{b_i}}{\partial \tau} \frac{\partial \Psi}{\partial \tau} + \Delta^{b_i} \frac{\partial^2 \Psi}{\partial \tau^2} \right]
\end{aligned} \tag{C.4}$$

Derivatives of Δ and Δ^{b_i} are given by

$$\frac{\partial \Delta}{\partial \delta} = (\delta - 1) \left\{ A_i \theta \frac{2}{\beta_i} [(\delta - 1)^2]^{\frac{1}{2\beta_i} - 1} + 2B_i a_i [(\delta - 1)^2]^{a_i - 1} \right\} \tag{C.5}$$

$$\begin{aligned}
\frac{\partial^2 \Delta}{\partial \delta^2} &= \frac{1}{\delta - 1} \frac{\partial \Delta}{\partial \delta} + (\delta - 1)^2 \times \left\{ 4B_i a_i (a_i - 1) [(\delta - 1)^2]^{a_i - 2} + 2A_i^2 \left(\frac{1}{\beta_i} \right)^2 \{ [(\delta - 1)^2]^{\frac{1}{2\beta_i} - 1} \}^2 \right. \\
&\quad \left. + A_i \theta \frac{4}{\beta_i} \left(\frac{1}{2\beta_i} - 1 \right) [(\delta - 1)^2]^{\frac{1}{2\beta_i} - 2} \right\}
\end{aligned} \tag{C.6}$$

$$\frac{\partial \Delta^{b_i}}{\partial \delta} = b_i \Delta^{b_i-1} \frac{\partial \Delta}{\partial \delta} \quad (\text{C.7})$$

$$\frac{\partial^2 \Delta^{b_i}}{\partial \delta^2} = b_i \left[\Delta^{b_i-1} \frac{\partial^2 \Delta}{\partial \delta^2} + (b_i - 1) \Delta^{b_i-2} \left(\frac{\partial \Delta}{\partial \delta} \right)^2 \right] \quad (\text{C.8})$$

$$\frac{\partial \Delta^{b_i}}{\partial \tau} = -2\theta b_i \Delta^{b_i-1} \quad (\text{C.9})$$

$$\frac{\partial^2 \Delta^{b_i}}{\partial \tau^2} = 2b_i \Delta^{b_i-1} + 4\theta^2 b_i (b_i - 1) \Delta^{b_i-2} \quad (\text{C.10})$$

$$\frac{\partial^2 \Delta^{b_i}}{\partial \delta \partial \tau} = -A_i b_i \frac{2}{\beta_i} \Delta^{b_i-1} (\delta - 1) [(\delta - 1)^2]^{\frac{1}{2\beta_i} - 1} - 2\theta b_i (b_i - 1) \Delta^{b_i-2} \frac{\partial \Delta}{\partial \delta} \quad (\text{C.11})$$

Derivatives of Ψ are given by

$$\frac{\partial \Psi}{\partial \delta} = -2C_i \Psi (\delta - 1) \quad (\text{C.12})$$

$$\frac{\partial^2 \Psi}{\partial \delta^2} = 2C_i \Psi [2C_i (\delta - 1)^2 - 1] \quad (\text{C.13})$$

$$\frac{\partial \Psi}{\partial \tau} = -2D_i \Psi (\tau - 1) \quad (\text{C.14})$$

$$\frac{\partial^2 \Psi}{\partial \tau^2} = 2D_i \Psi [2D_i (\tau - 1)^2 - 1] \quad (\text{C.15})$$

$$\frac{\partial^2 \Psi}{\partial \delta \partial \tau} = 4C_i D_i \Psi (\delta - 1) (\tau - 1) \quad (\text{C.16})$$

References

- Bishnoi, P. R., Hamaliuk, G. P., Robinson, D. B., October 1972. Experimental Heat Capacities of Nitrogen-Carbon Dioxide Mixtures at Elevated Pressures. The Canadian Journal of Chemical Engineering 50, 677–679.
- Brugge, H., Hwang, C.-A., Rogers, W., Holste, J., Hall, K., Lemming, W., Esper, G., Marsh, K., Gammon, B., 1989. Experimental Cross Virial Coefficients for Binary Mixtures of Carbon Dioxide with Nitrogen, Methane and Ethane at 300 and 320 k. Physica A 156, 382–416.
- Brugge, H. B., Holste, J. C., Hall, K. R., Gammon, B. E., Marsh, K. N., 1997. Densities of Carbon Dioxide + Nitrogen from 225 K to 450 K at Pressures up to 70 MPa. Journal of Chemical Engineering Data 42 (5), 903–907.
- Ely, J., Haynes, W., Bain, B., 1989. Isochoric (p, V_m, T) measurements on CO_2 and on $(0.982CO_2 + 0.018N_2)$ from 250 to 350 K at pressures to 35 MPa. Journal of Chemical Thermodynamics 21, 879–894.
- Gernert, G. J., 2013. A new helmholtz energy model for humid gases and ccs mixtures. Ph.D. thesis.
- Gernert, J., Jäger, A., Span, R., 2014. Calculation of phase equilibria for multi-component mixtures using highly accurate helmholtz energy equations of state. Fluid Phase Equilibria 375, 209–218.
- Hagermann, A., Rosenberg, P., Towner, M., Garry, J., Svedhem, H., Leese, M., Hathi, B., Lorenz, R., Zarnecki, J., 2007. Speed of sound measurements and the methane abundance in titan's atmosphere. Icarus 189 (2), 538–543.

- Hilsenrath, J., Beckett, C. W., Benedict, W. S., Lilla Fano, Harold J. Hoge, J. F. M. R. L. N. Y. S. T. H. W. W., 1955. Tables of Thermal Properties of Gases. National Bureau of Standards.
- Hinson, D. P., Jenkins, J. M., 1995. Magellan radio occultation measurements of atmospheric waves on venus. *Icarus* 114 (2), 310–327.
- Jenkins, J. M., Steffes, P. G., Hinson, D. P., Twicken, J. D., Tyler, G. L., 1994. Radio occultation studies of the venus atmosphere with the magellan spacecraft: 2. results from the october 1991 experiments. *Icarus* 110 (1), 79–94.
- Klimeck, R., May 1996. Entwicklung einer fundamentalgleichung für erdgase für das gas-und flüssigkeitsgebiet sowie das phasengleichgewicht. Ph.D. thesis, Ruhr-Universität Bochum.
- Kunz, O., Klimeck, R., Wagner, W., Jaeschke, M., 2007. The GERG-2004 wide-range equation of state for natural gases and other mixtures. *GERG TM 15 6* (557).
- Kunz, O., Wagner, W., 2012. The GERG-2008 wide-range equation of state for natural gases and other mixtures: an expansion of gerg-2004. *Journal of Chemical & Engineering Data* 57 (11), 3032–3091.
- Lemmon, E., May 1996. A Generalized Model for the Prediction of the Thermodynamic Properties of Mixtures including Vapor-Liquid Equilibrium. Ph.D. thesis, University of Idaho.
- Lemmon, E., Jacobsen, R., 1999. A Generalized Model for the Thermodynamic Properties of Mixtures. *International Journal of Thermophysics* 20 (3), 825–835.
- Linkin, V., Blamont, J., Devyatkin, S., Ignatova, S., Kerzhanovich, V., Lipatov, A., Malik, K., Stadnyk, B., Sanotskii, Y. V., Stolyarchuk, P., et al., 1987. Thermal structure of the atmosphere of venus from the results of measurements taken by landing vehicle vega-2. *Kosnicheskie Issledovaniya* 25 (5), 659–672.
- Mantovani, M., Chiesa, P., Valenti, G., Gatti, M., Consonni, S., 2012. Supercritical pressure–density–temperature measurements on CO_2-n_2 , CO_2-o_2 and CO_2-ar binary mixtures. *The Journal of Supercritical Fluids* 61, 34–43.
- Moroz, V., 1981. The atmosphere of venus. *Space Science Reviews* 29 (1), 3–127.
- Oyama, V., Carle, G., Woeller, F., Pollack, J., Reynolds, R., Craig, R., 1980. Pioneer venus gas chromatography of the lower atmosphere of venus. *Journal of Geophysical Research: Space Physics* 85 (A13), 7891–7902.
- Peplowski, P., Lawrence, D., 2016. Nitrogen content of venus’ upper atmosphere from the messenger neutron spectrometer. In: *Lunar and Planetary Science Conference*. Vol. 47. p. 1177.
- Seiff, A., Kirk, D. B., Young, R. E., Blanchard, R. C., Findlay, J. T., Kelley, G. M., Sommer, S. C., December 1980. Measurements of Thermal Structure and Thermal Constants in the Atmosphere of Venus and Related Dynamical Observations: Results From the Four Pioneer Venus Probes. *Journal of Geophysical Research* 85 (A13), 7903–7933.
- Seiff, A., Schofield, J., Kliore, A., Taylor, F., Limaye, S., Revercomb, H., Sromovsky, L., Kerzhanovich, V., Moroz, V., Marov, M. Y., 1985. Models of the structure of the atmosphere of venus from the surface to 100 kilometers altitude. *Advances in Space Research* 5 (11), 3–58.

- Sengers, J., Kayser, R., Peters, C., White Jr., J. (Eds.), 2000. Equations of State for Fluids and Fluid Mixtures. Vol. 5 of Experimental Thermodynamics. Elsevier.
- Span, R., Lemmon, E. W., Jacobsen, R. T., Wagner, W., Yokozeki, A., 2000. A Reference Equation of State for the Thermodynamic Properties of Nitrogen for Temperatures from 63.151 to 1000 K and Pressure to 2200 MPa. *Journal of Physical and Chemical Reference Data* 29 (6), 1361–1433.
- Span, R., Wagner, W., 1996. A New Equation of State for Carbon Dioxide Covering the Fluid Region from the Triple-Point Temperature to 1100 K at Pressures up to 800 MPa. *Journal of Physical and Chemical Reference Data* 25 (6).
- Staley, D. O., 1970. The Adiabatic Lapse Rate in the Venus Atmosphere. *Journal of the Atmospheric Sciences* 27, 219–223.
- Steffes, P. G., Jenkins, J. M., Austin, R. S., Asmar, S. W., Lyons, D. T., Seale, E. H., Tyler, G. L., 1994. Radio occultation studies of the venus atmosphere with the magellan spacecraft: 1. experimental description and performance. *Icarus* 110 (1), 71–78.
- STP-TS-012-1, 2012. Thermophysical Properties of Working Gases Used in Working Gas Turbine Applications. Standard, ASME Standards Technology, LLC, New York.
- Team, V. B. S., Seiff, A., 1987. Further information on structure of the atmosphere of venus derived from the vega venus balloon and lander mission. *Advances in space research* 7 (12), 323–328.
- Tillner-Roth, R., 1993. Die thermodynamischen eigenschaften von r152a, r134a und ihren gemischen. *Forschungsbericht des Deutschen Kälte-und Klimatechnischen Vereins* No. 41.
- Von Zahn, U., Kumar, S., Niemann, H., Prinn, R., 1983. Composition of the Venus Atmosphere. University of Arizona Press, pp. 299–430.
- Zasova, L. V., Moroz, V. I., Linkin, V. M., Khatuntsev, I. V., Maiorov, B. S., July 2006. Structure of the Venusian atmosphere from surface up to 100 km. *Cosmic Research* 44, 364–383.